

# Electronic properties and magnetism of iron at the Earth's inner core conditions

L. V. Pourovskii,<sup>1,2</sup> T. Miyake,<sup>3</sup> S. I. Simak,<sup>4</sup> A. V. Ruban,<sup>5</sup> L. Dubrovinsky,<sup>6</sup> and I. A. Abrikosov<sup>4</sup>

<sup>1</sup>*Centre de Physique Théorique, CNRS, École Polytechnique, 91128 Palaiseau, France*

<sup>2</sup>*Swedish e-science Research Centre (SeRC), Department of Physics, Chemistry and Biology (IFM), Linköping University, Linköping, Sweden*

<sup>3</sup>*Nanosystem Research Institute, AIST, Tsukuba 305-8568, Japan*

<sup>4</sup>*Department of Physics, Chemistry and Biology (IFM), Linköping University, Linköping, Sweden*

<sup>5</sup>*Department of Materials Science and Engineering,*

*Royal Institute of Technology, SE-10044, Stockholm, Sweden*

<sup>6</sup>*Bayerisches Geoinstitut, Universität Bayreuth, 95440 Bayreuth, Germany*

We employ state-of-the-art *ab initio* simulations within the dynamical mean-field theory to study three likely phases of iron (hexagonal close-packed, *hcp*, face centered cubic, *fcc*, and body centered cubic, *bcc*) at the Earth's core conditions. A non-Fermi liquid behaviour is observed for *bcc* Fe, and the correction to the electronic free energy due to correlations depends strongly on crystal structure. We predict that all three structures have sufficiently high magnetic susceptibility to stabilize the geodynamo. The strongest effect is observed in *bcc* Fe, where a large local magnetic moment of  $2.6 \mu_B$  still survives at 5800 K and 300 GPa.

PACS numbers:

Being the main component of the Earth's core, iron attracts significant attention from broad research community. Understanding its properties at ultra-high pressure and temperature, ranging from studies of the core structure to modeling the geodynamo is a long-term goal for the condensed matter physics, and is essential for explaining geochemical observations, seismic data, and for the theory of geomagnetism, to mention few examples. In spite of all previous theoretical and experimental efforts, the crystal structure and properties of solid Fe at the inner Earth core conditions remain a subject of intense debates. All three phases stable at low pressure-temperature conditions, namely, *hcp*, *fcc*, and *bcc*, have been suggested as possible crystal structures of iron or its alloys in the Earth inner core [1–5].

Theoretical simulations of iron at high pressures and temperatures generally rely on the picture of a wide-band metal with insignificant local correlations [3–6]. Indeed under compression the overlap between localized states increases and so does the bandwidth  $W$ , while the local Coulomb repulsion  $U$  between those states is screened more efficiently. The reduction of the  $U/W$  ratio is used to rationalize the absence of electronic correlations beyond the standard local density approximation (LDA) at high-pressure conditions. The increase of the  $3d$ -band width also results in the corresponding drop of the density of states at the Fermi energy leading to disappearance of the driving force for magnetism according to the Stoner criterion. Besides, even at the ambient pressure but at very high temperature  $T \gg T_c$  ( $T_c$  is the Curie temperature, which is 1043 K in  $\alpha$ -Fe) local magnetic moments are expected to be suppressed due to one-electron Stoner-type excitations. Thus, when extremely high pressure and temperature are simultaneously applied, disappearance of the local magnetic moment seems to be inevitable. Due to these considerations iron at the

Earth's inner core conditions has been modeled as non-magnetic within LDA-based approaches. The results of recent works of Sola et al. [7, 8], who applied fixed-node-approximation quantum Monte Carlo techniques to compute the equation of state and the melting temperature of *hcp* Fe at extreme conditions, are in good agreement with previous LDA-based simulations, thus strengthen the above argument, at least in the case of the *hcp* phase.

So, are electronic correlations important at extreme conditions, and can they lead to qualitatively new phenomena? To address this question we have investigated the impact of correlations on the electronic structure, magnetic properties and thermodynamic stability of iron by performing *ab initio* simulations of the *bcc*, *fcc* and *hcp* phases for the volume of  $7.05 \text{ \AA}^3/\text{atom}$  (corresponding to the pressures expected in the inner Earth core) and temperatures up to 5800 K. We employ a state-of-the-art fully self-consistent technique [9, 10] combining the full-potential linearized augmented plane-wave (FLAPW) band structure method with the dynamical mean-field theory (DMFT) [11] treatment of the on-site Coulomb repulsion between Fe  $3d$  states. A combination of LDA and DMFT has been applied earlier to study thermodynamic stability [12] and to describe magnetic properties [13] of paramagnetic *bcc* Fe at ambient pressure.

The strength of the on-site electron repulsion has been evaluated by the constrained random-phase-approximation (cRPA) method [14, 15]. From the corresponding LDA electronic structure, the partially screened Coulomb interaction  $W_r(r, r')$  was computed in the cRPA with  $d-d$  screening channels excluded to avoid double counting of screening effects. The Coulomb ( $U$ ) and exchange ( $J$ ) interaction matrices are then obtained as matrix elements of  $W_r(r, r')$  in a basis of localized Wannier functions representing Fe  $3d$  orbitals (see Ref. [15] for

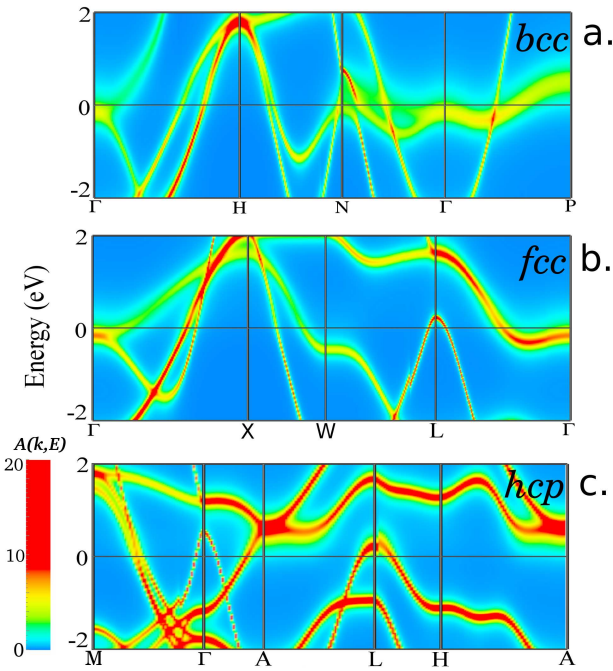


FIG. 1: (Color online) The LDA+DMFT  $k$ -resolved spectral function  $A(\mathbf{k}, E)$  ( $V_{at}/eV$ ) for *bcc* (a), *fcc* (b), and *hcp* (c) Fe at volume  $V_{at} = 7.05 \text{ \AA}^3/\text{atom}$  and temperature 5800 K. A non-quasiparticle  $e_g$  band is seen in the vicinity of the Fermi energy along the  $N - \Gamma - P$  path in (a).

details). The calculated Coulomb interaction matrices are well approximated by a spherically-symmetric form used in the subsequent calculations, with the parameter  $U$  (the Slater parameter  $F_0$ ) equal to 3.15, 3.04, and 3.37 eV and the Hund's rule coupling  $J$  equal to 0.9, 0.9 and 0.93 eV for *bcc*, *fcc*, and *hcp* phases, respectively.

In our LDA+DMFT calculations at the beginning of each iteration the eigenvalues and eigenvectors of the Kohn-Sham problem were obtained by the FLAPW code. Wannier-like functions for the Fe-3d shell were then constructed by projecting local orbitals onto a set of FLAPW Bloch states located within the energy window from -10.8 to 4 eV relative to the Fermi level (details of the projection procedure can be found in Ref. [9]). We then introduced the calculated local Coulomb interaction in the density-density form acting between those Wannier orbitals. We employed the around mean-field form [16] of the double counting correction term throughout. The resulting many-body problem has been solved within the DMFT framework by employing the exact Continuous-time hybridization expansion Quantum Monte-Carlo (CT-QMC) method [17] as the quantum impurity solver. The impurity problem was solved using  $5 \cdot 10^8$  CT-QMC moves with a measurement performed after each 200 moves. After completing the DMFT cycle we calculated the resulting density matrix

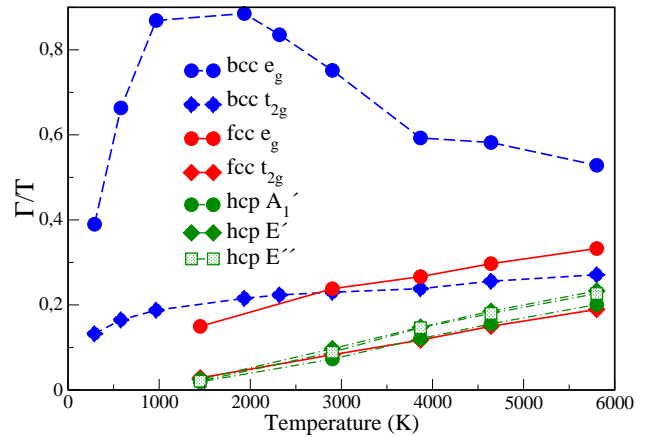


FIG. 2: (Color online) The ratio of the inverse quasiparticle lifetime  $\Gamma$  to temperature  $T$  vs.  $T$ . The solid red, dashed blue and dash-dotted green curves correspond to 3d states in *fcc*, *bcc*, and *hcp* Fe, respectively. They are split by the crystal field into  $t_{2g}$  (diamonds) and  $e_g$  (circles) representations in the cubic (*bcc* and *fcc*) phases, and two doubly-degenerate ( $E'$  and  $E''$ , shown by diamonds and squares, respectively) and one singlet ( $A_1'$ , circles) representations in the *hcp* phase, respectively. A non-linear behavior of  $\Gamma/T$  for *bcc* Fe  $e_g$  states is clearly seen.

in the Bloch states' basis, which was then used to recalculate the charge density in the next iteration as described in Ref. [10]. To obtain the spectral function at the real axis we employed a stochastic version of the Maximum Entropy method [18] for analytical continuation. In order to compute the magnetic susceptibility in uniform fields we performed LDA+DMFT simulations with the Kohn-Sham eigenstates split by the magnetic field  $H = 0.005 eV/\mu_B$  directed along the  $z$  axis, and then computed  $\chi = M/H$  from the resulting small magnetic moment  $M \sim 0.01 \mu_B$ .

In Fig. 2 we display the LDA+DMFT  $k$ -resolved spectral functions  $A(\mathbf{k}, E)$  for the three phases obtained for the temperature of 5800 K. First, one may notice that in *hcp* Fe the electronic states in the vicinity of the Fermi level  $E_F$  are sharp (their red color indicating high value of  $A(\mathbf{k}, E)$ ), hence  $\epsilon$ -Fe exhibits a typical behaviour of a Fermi-liquid with large quasi-particle life-times in the vicinity of  $E_F$ . In contrast, the *bcc* phase features a low-energy  $e_g$  band along the  $N - \Gamma - P$  path that is strongly broadened, thus indicating destruction of quasiparticle states. *fcc* Fe is in an intermediate state, with some broadening noticeable in the  $e_g$  bands at  $E_F$  in the vicinity of the  $\Gamma$  and  $W$  points.

To quantify the degree of non-Fermi-liquid behaviour we have evaluated the inverse quasiparticle life-time  $\Gamma = -Z \Im[\Sigma(i0^+)]$ , where the quasiparticle residue  $Z^{-1} = 1 - \frac{\partial \Im \Sigma(i\omega)}{\partial \omega} |_{\omega \rightarrow 0^+}$ , by extrapolating the imaginary-frequency self-energy  $\Sigma(i\omega)$  to zero. In the Fermi-liquid regime  $\Gamma$  scales as  $T^2$ , hence  $\Gamma/T$  vs.  $T$  is linear. In Fig. 2 we dis-

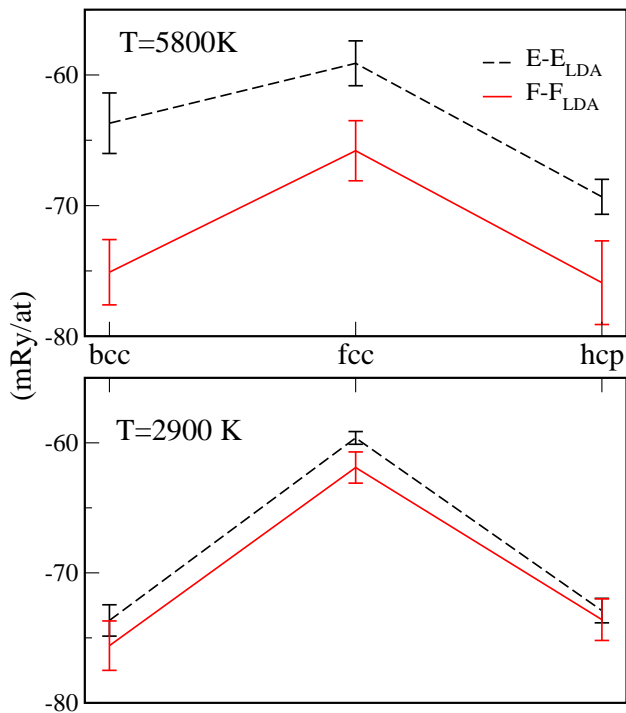


FIG. 3: (Color online) Many-body correction to the total (black dashed line) and free (red solid line) energy for the three phases of Fe at the volume of  $7.05 \text{ \AA}^3/\text{atom}$  at  $T=5800 \text{ K}$  (upper panel) and  $2900 \text{ K}$  (lower panel). The error bars are due to the CT-QMC stochastic error.

play the temperature evolution of  $\Gamma/T$  for the relevant irreducible representations of the Fe  $3d$  shell in all three phases. One may see that  $\Gamma/T$  in *hcp* Fe exhibits a linear increase typical for a Fermi liquid up to temperatures expected in the inner Earth core. In contrast,  $\Gamma/T$  for the *bcc* iron  $e_g$  states features a linear and steep rise for  $T < 1000 \text{ K}$  and then behaves non-linearly, indicating a non-coherent nature of those states at high temperatures. The *bcc* Fe  $t_{2g}$  and *fcc* Fe  $e_g$  electrons are in an intermediate situation with some noticeable deviations from the Fermi-liquid behaviour.

The tendency of *bcc*  $e_g$  states to a non-Fermi liquid behaviour has been noted before for ambient conditions and explained by a smaller effective bandwidth of the "localized"  $e_g$  band compared to the  $t_{2g}$  one [19]. We have evaluated the one-electron kinetic energy of the  $e_g$  and  $t_{2g}$  bands as  $E_b = \int_{-\infty}^{E_F} D(E)(E - C)dE$ , where  $D(E)$  is the corresponding LDA partial density of states (PDOS),  $C$  is the centralweight of the band and  $E_F$  is the Fermi energy. Resulting  $E_b$  for the  $e_g$  and  $t_{2g}$  bands in the *bcc* (*fcc*) phases are equal to  $-1.05$  ( $-1.01$ ) and  $-1.08$  ( $-1.20$ ) eV, respectively. One may see that the difference in kinetic energy between the  $e_g$  and  $t_{2g}$  bands in *bcc* Fe

is rather small and, in fact, even smaller than the corresponding difference in the *fcc* phase. Hence, it can hardly explain the observed qualitatively distinct non-Fermi liquid behaviour of the  $e_g$  states in *bcc*. It has been pointed out [20, 21] that a van Hove singularity in one of *bcc* Fe  $e_g$  bands leads to formation of a narrow peak in the corresponding PDOS in the vicinity of  $E_F$  [22]. A large peak in PDOS located at  $E_F$  leads to suppression of the low-energy hopping and to the corresponding enhancement of correlations, as has been recently pointed out for the case of  $\text{Sr}_2\text{RuO}_4$  [23]. A similar suppression is observed in the  $e_g$  hybridization function in *bcc* Fe [24].

Having demonstrated the impact of correlation effects on the Fe electronic structure we will now focus on its consequences for the Fe phase stability and magnetism at the inner Earth core conditions. In order to evaluate the impact of correlation effects on the relative stability of the three phases we have computed the corresponding correction to the fixed-lattice free energy by employing a coupling-constant integration approach (see in, e.g., Ref. [25]). We define the free energy  $F_\lambda = -\frac{1}{\beta} \ln \text{Tr}(\exp[-\beta(H_0 + \lambda H_1)])$  corresponding to a given value of the coupling  $\lambda \in [0 : 1]$ , where  $H_0$  is the one-electron (LDA) part of the Hamiltonian,  $H_1$  is the interacting part equal to the difference between the Hubbard term  $H_U$  and the double-counting correction  $E_{dc}$ . The coupling constant integration leads to the following expression for the many-body correction to the electronic free energy:

$$\Delta F = F - F_0 = \int_0^1 \frac{\langle \lambda H_1 \rangle_\lambda}{\lambda} d\lambda \quad (1)$$

In derivation of Eq. 1 we neglected the  $\lambda$  dependence of the one-electron part, and, hence, the charge density renormalization due to many-body effects. However, we verified that the difference in the total energies obtained with and without the charge density self-consistency is small, and the correction to the total energy due to the charge density self-consistency is within our error bars.

To obtain  $\Delta F$  we have computed  $\frac{\langle \lambda H_1 \rangle_\lambda}{\lambda}$  for a discret set of values of  $\lambda$  ranging from 0 to 1 by performing LDA+DMFT simulations with the Coulomb interaction scaled accordingly and evaluating  $\langle \lambda H_U \rangle_\lambda$  in accordance with the Migdal formula [26]. Then we integrated  $\frac{\langle \lambda H_1 \rangle_\lambda}{\lambda}$  over  $\lambda$  numerically in order to obtain  $\Delta F$  and its error bar.

The resulting many-body correction to the electronic free energy is displayed in Fig. 3 for temperatures of  $2900 \text{ K}$  and  $5800 \text{ K}$ . There we also show the corresponding correction to the total energy  $\Delta E = E_{DMFT} - E_{LDA}$ , where  $E_{DMFT}$  was computed in accordance with Eq. (3) of Ref. [10]. Within our error bars the magnitude of  $\Delta F$  is the same for *bcc* and *hcp* Fe, which are suggested as stable phases of iron[4] and iron-based alloys [1, 2]

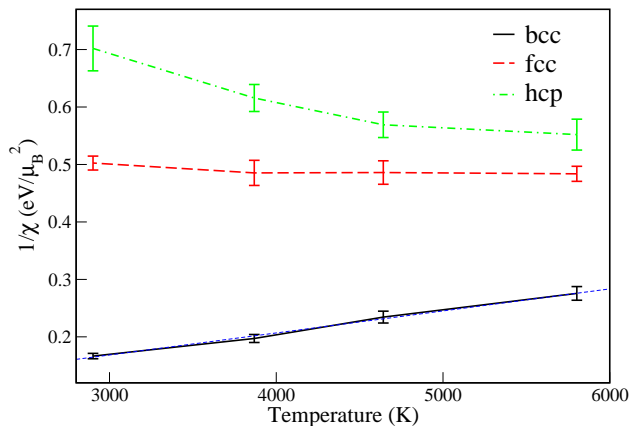


FIG. 4: (Color online) The inverse of uniform magnetic susceptibility in paramagnetic state versus temperature. The error bars are due to the CT-QMC stochastic error. The blue dashed line is a fit of the bcc Fe inverse susceptibility to the Curie-Weiss law.

at the Earth’s inner core conditions. The magnitude of  $\Delta F$  is substantially smaller in the case of *fcc* Fe, showing that the many-body correction is strongly structure-dependent. One may also notice that the entropic contribution (i.e. the difference  $T\Delta S = \Delta E - \Delta F$ ) becomes much more significant at the higher temperature, and its contribution is almost twice larger in the case of *bcc* Fe compared to the *hcp* and *fcc* phases.

The application of the LDA+DMFT theory has the most important consequences for the understanding of magnetic properties of Fe at the Earth’s core conditions. In Fig. 4 we display the temperature evolution of the inverse uniform magnetic susceptibility  $\chi^{-1}$ . One may notice that in the *fcc* and *hcp* phases the susceptibility exhibits a temperature-independent Pauli behaviour expected in a Fermi liquid [27]. In contrast,  $\chi^{-1}$  of *bcc* Fe features a clear linear temperature dependence. We have fitted  $\chi^{-1}$  versus  $T$  of the *bcc* phase to the Curie-Weiss law  $\chi^{-1} = \frac{1}{3} \frac{\mu_{eff}^2}{T + \Theta}$  and obtained  $\mu_{eff} = 2.6 \mu_B$  and  $\Theta = 1396 K$ , which explicitly shows that *local magnetic moments* survive in this phase at the pressure  $\sim 300$  GPa and temperature of 5800 K, corresponding to the conditions in the Earth’s inner core.

The value of  $\Theta$  gives an estimate for the coherence scale in *bcc* Fe. It is in qualitative agreement with the value of  $\sim 1000$  K for the coherence scale extracted from the temperature evolution of the inverse quasiparticle lifetime  $\Gamma$ , see above. Below the coherence temperature  $\Theta$  *bcc* Fe is expected to evolve into a paramagnetic Fermi liquid with a Pauli behaviour of the susceptibility. Thus, the Curie-Weiss behavior of magnetic susceptibility and the existence of local magnetic moments cannot be observed in room temperature experiments. The effect predicted in our calculations is induced by ultra-high temperature

in the Earth’s core.

The value of calculated uniform susceptibility in SI units at temperature  $T=5800$  K is equal to  $1.7 \cdot 10^{-4}$ ,  $2.0 \cdot 10^{-4}$ , and  $3.5 \cdot 10^{-4}$  for *hcp*, *fcc*, and *bcc* Fe, respectively. We would like to underline that our calculated uniform magnetic susceptibilities in all three phases of Fe are sufficiently high to be important for models of the Earth core dynamics and geodynamo (see e.g. Ref. [28]). An inner core with a paramagnetic susceptibility in the range  $10^{-3} - 10^{-4}$  SI units, and with a paramagnetic relaxation time acting slower than field changes coming from the outer core, could also attenuate short frequency fluctuations and become an important factor stabilizing the geodynamo[29], just as an electrically conducting inner core could stabilize the geodynamo because the inner core would have a magnetic diffusion constant independent of the outer core[30, 31].

In conclusion, we have carried out a theoretical investigation of the role of electronic correlations in Fe at the inner Earth core conditions using a fully self-consistent LDA+dynamical mean-field theory approach. We considered all three crystal structures, *bcc*, *fcc* and *hcp*, that have been suggested as stable solid phases for the inner core and found that the *fcc* and *hcp* phases remain in a Fermi-liquid state, while *bcc* Fe features a non-Fermi-liquid behaviour. This incoherent state of *bcc* Fe is due to a large peak in its one-electron density of states suppressing the low-energy hopping and thus increasing the strength of correlations. We have evaluated a correction to the electronic free energy due to many-body effects and found that it is strongly structurally-dependent, penalizing the *fcc* phase. This structurally-dependent correction will affect the shape of the electronic free energy “landscape” and, consequently, the forces arising due to a lattice distortion in a given phase. Most interestingly, we predict that a local magnetic moment exists in the *bcc* phase at the inner core conditions and that magnetic susceptibilities in all three phases of Fe are sufficiently high to stabilize geodynamo. Thus, new models of geodynamo as well as the core structure and elasticity should include the magnetism of the Earth’s core, the effect of which so far was never considered.

We are grateful to J. Mravlje, V. Vildosola, and A. Georges for useful discussions. We acknowledge the funding provided by Swedish e-science Research Centre (SeRC), Swedish Research Centre for Advanced Functional Materials (AFM), Linköping Linnaeus Initiative for Novel Functional Materials (LiLI-NFM), SRL grant 10-0026 from the Swedish Foundation for Strategic Research (SSF), the Swedish Research Council (VR) grant 621-2011-4426 and PHD DALEN 2012 project 26228RM as well as financial support from German Science Foundation (DFG) and German Ministry for Education and Research (BMBF). Calculations have been performed using the facilities of the National Supercomputer Centre in Linköping (NSC) and High Performance Computing

Center North (HPC2N) at Swedish National Infrastructure for Computing (SNIC).

- 
- [1] J.-F. Lin, D. L. Heinz, A. J. Campbell, J. M. Devine, and G. Shen, *Science* **295**, 313 (2002).
- [2] L. Dubrovinsky, N. Dubrovinskaia, O. Narygina, I. Kantor, A. Kuznetsov, V. B. Prakapenka, L. Vitos, B. Johansson, A. S. Mikhaylushkin, S. I. Simak, and I. A. Abrikosov, *Science* **316**, 1880 (2007).
- [3] A. B. Belonoshko, R. Ahuja, and B. Johansson, *Nature* **424**, 1032 (2003).
- [4] L. Vočadlo, D. Alfè, M. J. Gillan, I. G. Wood, J. P. Brodholt, and G. D. Price, *Nature* **424**, 536 (2003).
- [5] A. S. Mikhaylushkin, S. I. Simak, L. Dubrovinsky, N. Dubrovinskaia, B. Johansson, and I. A. Abrikosov, *Phys. Rev. Lett.* **99**, 165505 (2007).
- [6] L. Stixrude, *Phys. Rev. Lett.* **108**, 055505 (2012).
- [7] E. Sola, J. P. Brodholt, and D. Alfè, *Phys. Rev. B* **79**, 024107 (2009).
- [8] E. Sola and D. Alfè, *Phys. Rev. Lett.* **103**, 078501 (2009).
- [9] M. Aichhorn, L. Pourovskii, V. Vildosola, M. Ferrero, O. Parcollet, T. Miyake, A. Georges, and S. Biermann, *Phys. Rev. B* **80**, 085101 (2009).
- [10] M. Aichhorn, L. Pourovskii, and A. Georges, *Phys. Rev. B* **84**, 054529 (2011).
- [11] A. Georges, G. Kotliar, W. Krauth, and M. J. Rozenberg, *Rev. Mod. Phys.* **68**, 13 (1996).
- [12] I. Leonov, A. I. Poteryaev, V. I. Anisimov, and D. Vollhardt, *Phys. Rev. Lett.* **106**, 106405 (2011).
- [13] A. I. Lichtenstein, M. I. Katsnelson, and G. Kotliar, *Phys. Rev. Lett.* **87**, 067205 (2001).
- [14] F. Aryasetiawan, M. Imada, A. Georges, G. Kotliar, S. Biermann, and A. I. Lichtenstein, *Phys. Rev. B* **70**, 195104 (2004).
- [15] T. Miyake and F. Aryasetiawan, *Phys. Rev. B* **77**, 085122 (2008).
- [16] M. T. Czyżyk and G. A. Sawatzky, *Phys. Rev. B* **49**, 14211 (1994).
- [17] E. Gull, A. J. Millis, A. I. Lichtenstein, A. N. Rubtsov, M. Troyer, and P. Werner, *Rev. Mod. Phys.* **83**, 349 (2011).
- [18] K. S. D. Beach, cond-mat/0403055 (unpublished).
- [19] A. A. Katanin, A. I. Poteryaev, A. V. Efremov, A. O. Shorikov, S. L. Skornyakov, M. A. Korotin, and V. I. Anisimov, *Phys. Rev. B* **81**, 045117 (2010).
- [20] R. Maglic, *Phys. Rev. Lett.* **31**, 546 (1973).
- [21] V. Y. Irkhin, M. I. Katsnelson, and A. V. Trefilov, *Journal of Physics: Condensed Matter* **5**, 8763 (1993).
- [22] See plots of LDA DOS for all three structures at the volume of  $7.05 \text{ \AA}^3/\text{atom}$  in Supplemental Material Fig. S1.
- [23] J. Mravlje, M. Aichhorn, T. Miyake, K. Haule, G. Kotliar, and A. Georges, *Phys. Rev. Lett.* **106**, 096401 (2011).
- [24] See plots of the hybridization functions in *bcc* and *fcc* Fe at the volume of  $7.05 \text{ \AA}^3/\text{atom}$  in Supplemental Material Fig. S2 .
- [25] P. Nozières, *Theory of interacting Fermi systems* (W. A. Benjamin, New York, 1963).
- [26] We calculated  $\frac{\langle \lambda H_1 \rangle_\lambda}{\lambda} |_{\lambda=0}$  analytically, as in this case it is equal to the Hartree-Fock approximation to  $\langle H_U \rangle$  computed with the LDA density matrix minus the double-counting correction. The resulting value of  $\frac{\langle \lambda H_1 \rangle_\lambda}{\lambda} |_{\lambda=0}$  is small, of order of 0.1 mRy.
- [27] A small decrease in  $\chi$  at lower temperatures observed in *hcp* Fe is due to a dip in its one-electron DOS in the vicinity of the Fermi level, see Supplemental Material Fig. S1.
- [28] J. Aubert, S. Labrosse, and C. Poitou, *Geophys. J. Int.* **169**, 1414 (2009).
- [29] B. M. Clement and L. Stixrude, *Earth And Planetary Science Letters* **130**, 75 (1995).
- [30] S. Gilder and J. Glen, *Science* **279**, 72 (1998).
- [31] R. Hollerbach and C. Jones, *Nature* **365**, 541 (1993).

## Supplemental Material

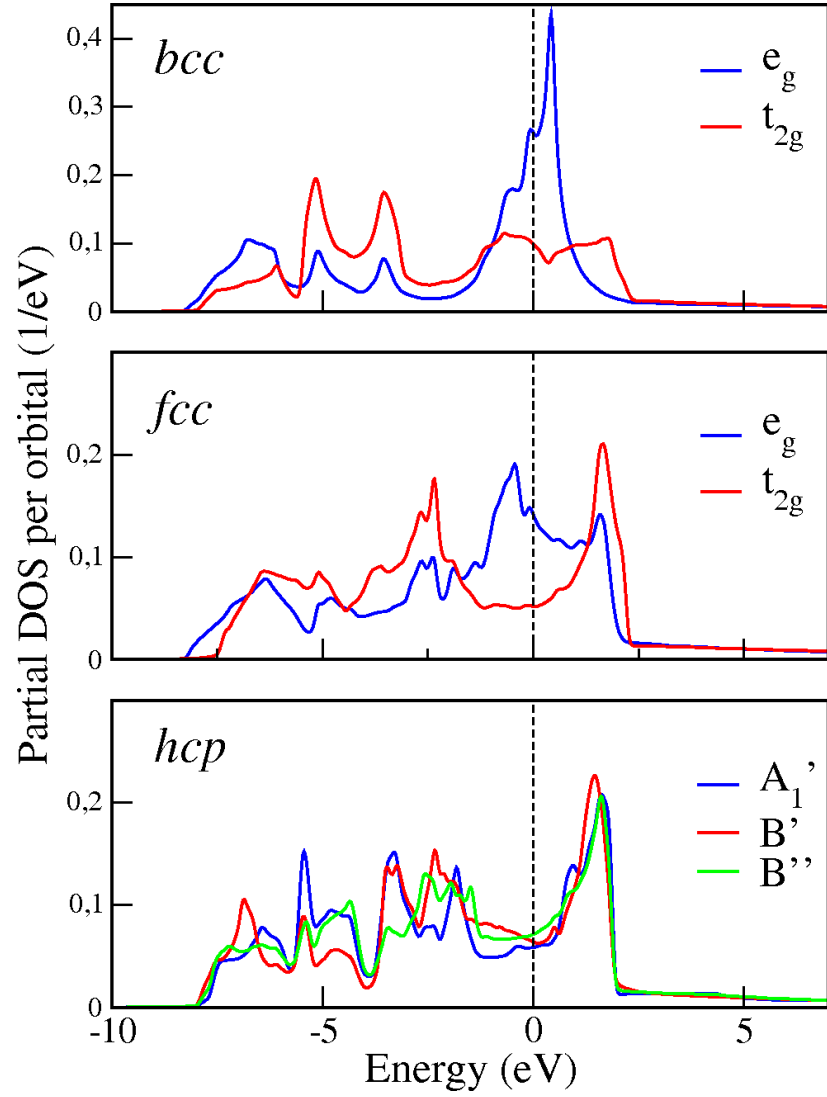


FIG. S1: Partial LDA densities of states (PDOS) for the irreducible representations of Fe 3d states for the three phases at the volume  $7.05 \text{ \AA}^3/\text{atom}$ . The large peak in the vicinity of  $E_F$  in bcc Fe  $e_g$  PDOS is due to a van Hove singularity.

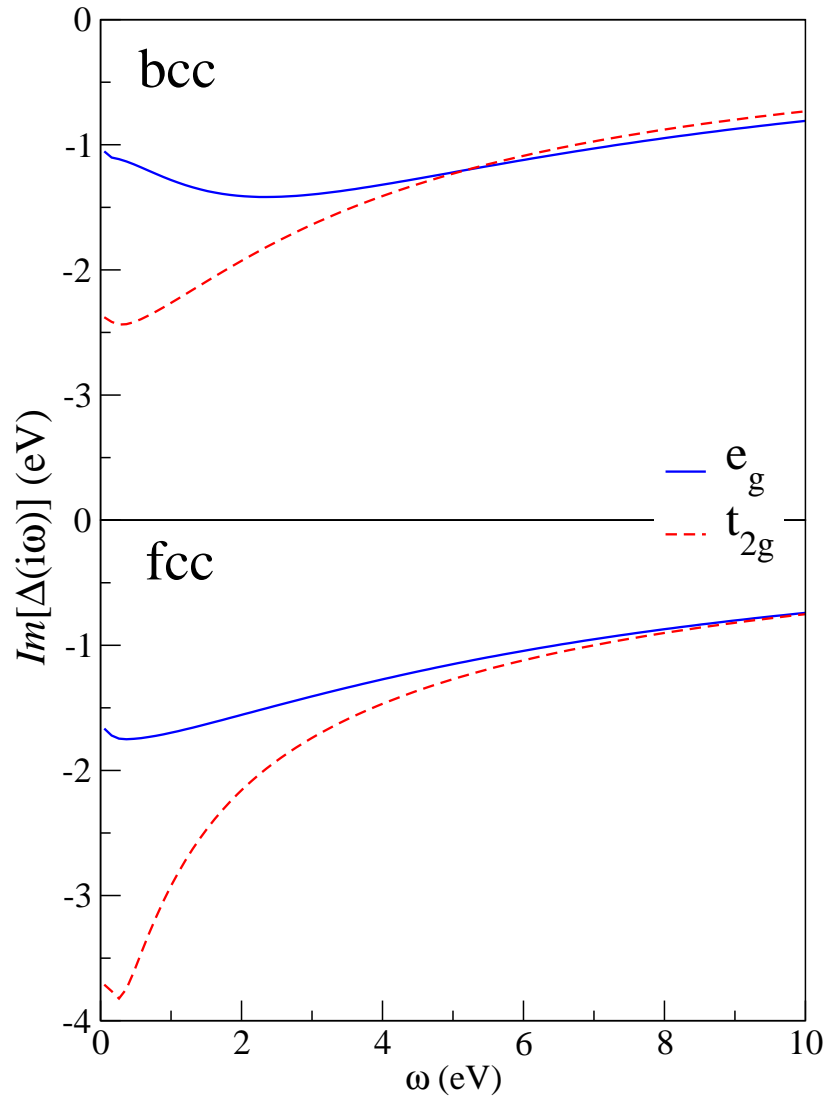


FIG. S2: Imaginary part of the hybridization function  $\Delta$  versus imaginary frequency for the  $e_g$  and  $t_{2g}$  states at the first DMFT iteration. In *bcc* Fe one may clearly see a decrease in  $|\Im\Delta(i\omega)|$  of the  $e_g$  states at  $\omega < 2$  eV. However, at higher energies ( $\omega > 5$  eV) the  $e_g$  hybridization function decays slowly and becomes larger than the  $t_{2g}$  one. The overall one-electron kinetic energies of  $e_g$  and  $t_{2g}$  states in *bcc* Fe have similar values as explained in the main text. In contrast, in the *fcc* phase  $|\Im\Delta(i\omega)|$  grows monotonously with decreasing  $\omega$  for both  $e_g$  and  $t_{2g}$ .